



The impact of localized grey matter damage on neighboring connectivity: posterior cortical atrophy and the visual network

Haya Glick-Shames¹ · Yael Backner¹ · Atira Bick¹ · Noa Raz¹ · Netta Levin¹

Published online: 25 August 2018

© Springer Science+Business Media, LLC, part of Springer Nature 2018

Abstract

Posterior cortical atrophy (PCA), a localized neurodegenerative syndrome involving the occipito-parietal cortices, can serve as a good model to elaborate on the consequence of a localized damage on the anatomical and functional connectivity within an affected system. Ten PCA patients and 14 aged-matched controls were enrolled. Structural connectivity was measured via Diffusion Tensor Imaging (DTI) and probabilistic tractography. The optic tracts and radiations and the splenial fibers were delineated and their microstructural properties were evaluated. Functional connectivity was measured by resting state functional MRI (rsfMRI). Voxel-based morphometry (VBM) was used to assess atrophy. Dorsal stream visual functions were tested and correlation between these behavioral data, volume measures, white matter integrity and connectivity were examined. Impaired white matter integrity was evident in patients' optic radiations and occipito-callosal fibers, in the segments located in close proximity to the occipital cortex, suggesting a localized damage. Degeneration did not proceed to the optic tracts, opposing trans-synaptic changes. rsfMRI revealed reduced connectivity within the visual network and between the visual and other related areas such as the frontal eye field. Correlations were found between grey matter volume and spatial perception abilities and between the integrity of the affected fibers and motion perception. White matter involvement in PCA seems to be grey matter dependent. Functional connectivity, on the other hand, showed a more diffuse pattern of damage. Correlations were found between the integrity of the affected fibers and patients' visual abilities suggesting that fiber integrity plays a role in determining behavioral manifestation.

Keywords Diffusion tensor imaging · Functional connectivity · Motion perception · Resting state fMRI and visual cortex

Introduction

Though Alzheimer's disease (AD) is the most well-known and studied regional grey matter (GM) volume reduction disease (Gress 2001), white matter (WM) involvement has also repeatedly been suggested both in typical AD as well as in its different variants (Canu et al. 2012).

WM damage was reported as a general phenomenon (Bartzokis 2004; de la Monte 1989; Burns et al. 2005) but also as a more localized one, in the parahippocampal regions,

reflecting the topography of GM loss. The extent of WM involvement has also been suggested as an indicator of disease severity (Canu et al. 2012). From these findings of WM involvement in degenerative disease two potential pathophysiological mechanisms arise: the first derives from primary oligodendrocyte and myelin damage which mainly affects heavily-wired areas such as the higher cognitive and memory regions (Bartzokis 2004); the second is projected by GM pathology (Canu et al. 2012; Frisoni et al. 2007). Another possibility, that can stand on its own or play a part in one of the other theories, is that the disease spreads trans-neuronally, through long WM connections (Caso et al. 2015).

Posterior Cortical Atrophy (PCA) is considered a visual variant of AD (Kaeser et al. 2015), mainly involving occipito-parietal regions, manifesting with visual perceptual skills deterioration (Benson et al. 1988). We recently suggested behavioral and cortical evidence pinpointing the damage to the dorsal aspects of perception. Our PCA patient cohort exhibited higher dorsal stream-related functional

Electronic supplementary material The online version of this article (<https://doi.org/10.1007/s11682-018-9952-7>) contains supplementary material, which is available to authorized users.

✉ Netta Levin
netta@hadassah.org.il

¹ fMRI lab, Neurology Department, Hadassah-Hebrew University Medical Center, POB 12000, 91120 Jerusalem, Israel

impairments, including simultant perception, image orientation, figure-from-ground segregation, closure and spatial orientation. In accordance with the behavioral findings, functional magnetic resonance imaging (fMRI) revealed intact activation in the ventral visual regions of face and object perception while more dorsal aspects of perception, including motion and gestalt perception, revealed impaired patterns of activity (Shames et al. 2015).

Beyond this distinct manifestation, the related network, the human visual system, is well defined, in contrast to other neuronal systems prone to degeneration. These characteristics put forward PCA as a fine model for tracking tissue degeneration and reorganization.

Herein we will utilize voxel based morphometry (VBM), diffusion tensor imaging (DTI) and fMRI to study the effect of localized GM damage on structural and functional connectivity within the visual network, known to be selectively affected in PCA. The association with behavioral manifestations will also be examined, to better define the role of connectivity in neurodegenerative disease and its effects on function.

Materials and methods

Subjects

Ten PCA patients (4 females), aged 63.3 ± 8.15 years (average \pm SD) were studied, based on the criteria described in the meta-analysis of Alves et al. (2013) and the first two levels of the consensus criteria described by Crutch et al. (2017). Average time from initial symptoms was 2.88 ± 0.64 years. Fourteen aged-matched healthy volunteers (6 females, aged 60.86 ± 7.17 years) were enrolled as a control group.

The Hadassah Hebrew University Medical Center Ethics Committee approved the experimental procedure. Written informed consent was obtained from all subjects.

Experimental design

Neuropsychological evaluation Visual Neuropsychological evaluation of dorsal stream-related visual functions included the Rey's Complex Figure Copy Test (Lieberman et al. 1994) to assess visuo-motor integration; the Gollin picture (Gollin 1960) and Hooper visual organization tests (Greve et al. 2000) to assess visual closure abilities; the "15-Object Test" based on Poppelreuter-Ghent's overlapping figures test (Della Sala et al. 1995; Pillon et al. 1989) to assess figure-ground segregation abilities; and the motion coherence test (Braddick et al. 2003) to assess motion perception.

This battery of tests was selected based on our previous findings of a specific dorsal stream-related functional impairment in PCA patients (Shames et al. 2015).

MRI data

MRI data were acquired on a 3-Tesla scanner (4 patients and 6 controls on Siemens Trio; 6 patients and 8 controls on Siemens Skyra) using a 32-channel standard head-coil.

MRI sequences included high-resolution T1-weighted images (minimum echo time [TE], flip angle 9° , repetition time [TR] = 2300 ms, voxel size of $1 \times 1 \times 1$ mm).

For **VBM** we used the Computational Analysis Toolbox (CAT 12, Jena University hospital), an extension of SPM12 (Wellcome Department of cognitive Neurology). Data was segmented into grey matter (GM), WM and cerebral spinal fluid (CSF), and normalized to Montreal Neurological Institute (MNI) space. Data quality was checked for homogeneity (all scans were within one standard deviation of homogeneity). The GM of the two groups was compared using a two sample *t* test, with total intracranial volume (TIV), scanner and age as covariates. Regions showing significant reduction in the patients' group were defined as atrophied foci.

DTI data were acquired using a diffusion-weighted imaging sequence, (single-shot, spin-echo, TE = 94 ms, TR = 7127–8224 ms, FOV = 260×260 mm, matrix = 128×128 , 52–60 axial slices, 2-mm-thick slices, $b = 0$ and $b = 1000$ s/mm²). The high *b*-value was obtained by applying gradients along 64 different diffusion directions.

DTI image processing and fiber tractography were performed using the mrVista package (Vista lab, Stanford University) (see *Supplementary Methods* for preprocessing details). The post-chiasmatal afferent visual pathways, including optic tracts and optic radiations, were delineated using the probabilistic Contrack algorithm which identifies the most likely pathway between two regions of interest (ROIs) (Sherbondy et al. 2008); the chiasm and lateral geniculate nuclei (LGN) for the *optic tracts* and the LGN and calcarine sulcus (V1) for the *optic radiations*. ROIs were anatomically defined in each subject on co-registered T1 maps.

The fiber tensors were fitted using a least-squares algorithm and each tensor underwent eigenvalue decomposition in order to derive measures of fractional anisotropy (FA), diffusion parallel (axial diffusivity, AD) and diffusion perpendicular (radial diffusivity, RD) to the primary fiber direction. These measurements were then resampled along the tracts in 30 or 50 equidistant points (relative to the length of the fiber bundle; 30 points in the optic tracts and 50 points in the optic radiations). This enabled the combination of measures from different subjects. To avoid partial volume effects with non-white matter, a core fiber was defined along the mean position of the defined sampling points (Yeatman et al. 2012).

The *occipital callosal* (splenial) fibers were tracked using a deterministic streamlines tracing technique (STT), according to MrVista default parameter (FA threshold 0.15, minimum angle 30°) algorithm as described previously (Huang et al.

2005). Briefly, the corpus callosum as a whole was used as one ROI and a second ROI was defined in the deep WM of the occipital lobe. FA, AD and RD were also extracted for these fibers.

Additionally, the relative volume of the corpus callosum taken by the occipital fiber group was measured over the five central sagittal slices and compared between the study cohorts.

Resting state fMRI measurements were obtained with an echo-planar imaging sequence, (TR/TE = 2250/30 ms, FOV = 218×218 mm², matrix 64×64 , 37 slices, slice thickness 3.4 mm). Data analysis was performed using the BrainVoyager QX software package (Brain Innovation, Maastricht, The Netherlands).

Functional images were co-registered to the anatomical images through trilinear interpolation and were transformed into MNI space (Evans et al. 1993) (see *Supplementary Methods* for preprocessing details).

For each subject, a seed region composed of the left and right V1 was defined. This was demarcated as a 10 mm cube around the central point of BA17, as defined by the Yale atlas of Brodmann areas (Lacadie et al. 2008) (See *Supplementary Methods* for further details). Individual connectivity maps from this seed region were generated for each subject and were then averaged across subjects using a hierarchical random effect model, allowing a generalization of the results to the population level.

Connectivity levels within and outside the visual network were evaluated on individual V1 seed-region maps. t-values for pre-defined regions, detailed below, were extracted and used as the connectivity levels between primary visual cortex and these regions. Regions included the LGN, lateral occipital complex (LOC), middle temporal area (MT), fusiform gyrus (FFG), lateral intraparietal cortex (LIP), frontal eye field (FEF), and primary motor area (M1).

Statistical analysis

For VBM analysis, threshold was set to p value <0.01 , corrected for family-wise error (FWE). Cluster-wise p value threshold was set to 0.05, corrected for false discovery rate (FDR). Coordinates were reported in the MNI standard anatomical space. Correlation analyses to other measures were conducted using SPSS® version 24.0 (IBM Corporation, Armonk, NY, USA).

For DTI analysis differences between diffusivity measures in PCA patients and controls were studied twofold. Firstly, the mean FA, AD, and RD of each tract were compared, using a two-tailed Student's t test. Significance level was defined as $p < 0.05$. Secondly, differences between the groups *along* the tract profiles were assessed. Given the high correlation degree between adjacent points on the tract, a

permutation-based multiple comparisons correction was used as in (Reiner et al. 2003).

For resting state fMRI analysis differences in connectivity levels between primary visual cortex and other visual regions were evaluated among the groups. A student t -test was performed on the obtained t -values from each ROI.

For correlation analysis, we first assessed the effect of GM atrophy on structural and functional measurements as well as on behavioral manifestations. Correlation between the volumes of atrophied foci (as defined by VBM) and the other measures were evaluated.

Then we evaluated the possible correlations between functional connectivity, structural connectivity and visual behavioral measurements using the non-parametric Kendall regression analysis. The FA, AD and RD of the visual pathways and connectivity measures (t - values) in the various visual areas were used as independent variables and the individual behavioral measurements were inserted as dependent variables. To avoid the possible effects of age and disease duration, those values were used as covariates of no interest using a partial correlation analysis. Correction for multiple comparisons by FDR correction was applied (Reiner et al. 2003). To assess the involvement of GM atrophy on the above correlations, we repeated the analysis adding the GM volume as a covariant.

Results

Neuropsychological evaluation

Dorsal-related visual function deficits are observed in the patient cohort Compared with adult norms, patients had lower results on the Rey figure copy test (7.375 ± 8.54 attributes were correctly copied vs. average adult norms of 29.32 ± 4.63 (Shin et al. 2006)); the Hooper test (7.75 ± 5.17 items recognized vs. 15.75 ± 5.89 (Tamkin and Jacobsen 1984)); the Gollin visual closure test (4.04 ± 1.06 attributes needed to identify the object vs. 1.95 ± 0.62 (Gollin 1960)); and the “15 Object Test” of overlapping figs. (5.71 ± 4.16 different items were recognized in a tangled image vs. 13.82 ± 1.08 (Alegret et al. 2009)). Patients also showed difficulty identifying motion coherence and were able to recognize movement direction only when a high percentage of dots were moving together in the same direction ($37.14 \pm 31.94\%$ coherence needed for identification of motion direction vs. $5.05 \pm 1.09\%$ in a group of controls we described in an earlier paper (Shames et al. 2015)).

VBM measurements

Atrophy is seen in the associative visual cortex (Fig. 1) Significant differences were found between groups in GM volume ($p = 0.001$) and CSF volume ($p = 0.004$). No

significant differences were found in TIV ($p = 0.33$) or in WM volume ($p = 0.098$). After correction of family wise estimation (FWE) ($p \leq 0.05$) three clusters of significant volume differences (atrophied foci) were found within the associative visual cortex: in the right and left anterior occipital lobe and in the right middle temporal area (cluster size corrected for FDR $p \leq 0.05$).

See Table 1 for MNI coordinates of the atrophied foci.

Diffusivity measurements

Optic tracts diffusivity measurements are preserved (Fig. 2)

No differences were evident for the average optic tracts' FA, RD and AD between the PCA and control groups (Left: $p = 0.53$, $p = 0.57$, and $p = 0.63$; Right $p = 0.39$, $p = 0.32$, and $p = 0.39$, respectively). Similar results were evident when analyzing fractional and directional diffusivities along the fibers; i.e. PCA and control groups did not differ in any diffusivity values at any point along the optic tract.

Optic radiations integrity is impaired mainly in their posterior parts (Fig. 3)

Addressing average diffusivity measurements demonstrated reduced FA in PCA patients' as compared to controls on the left side ($p = 0.02$). The averaged FA on the right optic radiation did not differ between the groups ($p = 0.21$). The averaged RD and AD did not differ between the

groups on either side ($p = 0.87$ and $p = 0.13$, for the left and right RD; $p = 0.76$ and $p = 0.09$ for the left and right AD).

When analyzing diffusivity along the tract, reduced FA (corrected for multiple comparisons), was found along points 42–50 on the left optic radiation and along points 33–47 on the right optic radiation. Increased RD was evident on the left optic radiation along points 29–36 and point 47. No significant differences were observed in the right optic radiation at any point. No significant differences were observed in AD at any point along either optic radiation.

Thus, optic radiations' integrity differs between patients and controls, as reflected by their reduced FA, mainly due to increased RD in the more posterior part of the bundle. Changes are more prominent in the left side.

Occipital callosal fibers diffusivity differs only in their lateral parts (Fig. 4)

No significant differences were evident for the average occipito-callosal fibers' FA, RD and AD when taking into account all points along either tract (Left: $p = 0.19$, $p = 0.18$ and $p = 0.35$; Right: $p = 0.77$, $p = 0.52$, $p = 0.32$ for FA, RD, and AD, respectively).

Analyzing diffusivity along the tracts revealed reduced FA on the left side, along points 11–22. No points reached significance on the right. Elevated RD was seen on both sides: along points 13–19 on the left side and along points 16–26 on the right side. No differences were observed in AD at any point

Fig. 1 Atrophied foci.

Visualization of the Voxel-based morphometry analysis shown as highlighted areas that represent atrophied foci in PCA group compared to controls, overlaid on a standard 3D SPM brain template

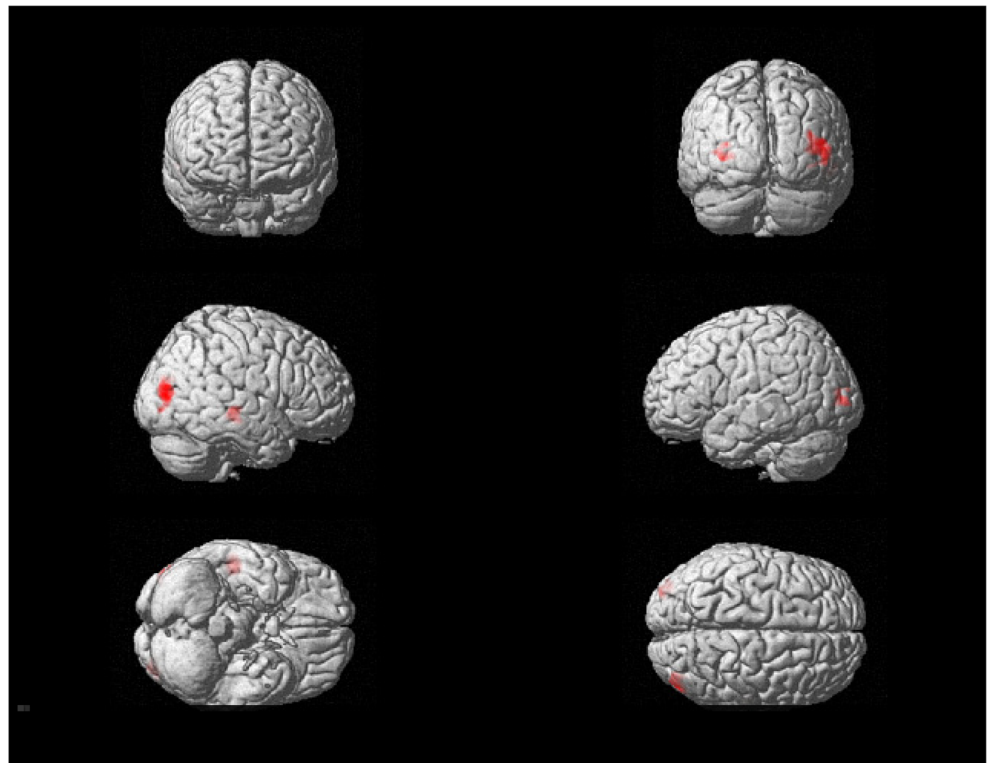


Table 1 Atrophied foci (per VBM) characteristics: Estimated location, size, p values (corrected for family wise estimation, FWE) and peak MNI-coordinates, of the atrophied foci that were found in the PCA group as compared to controls

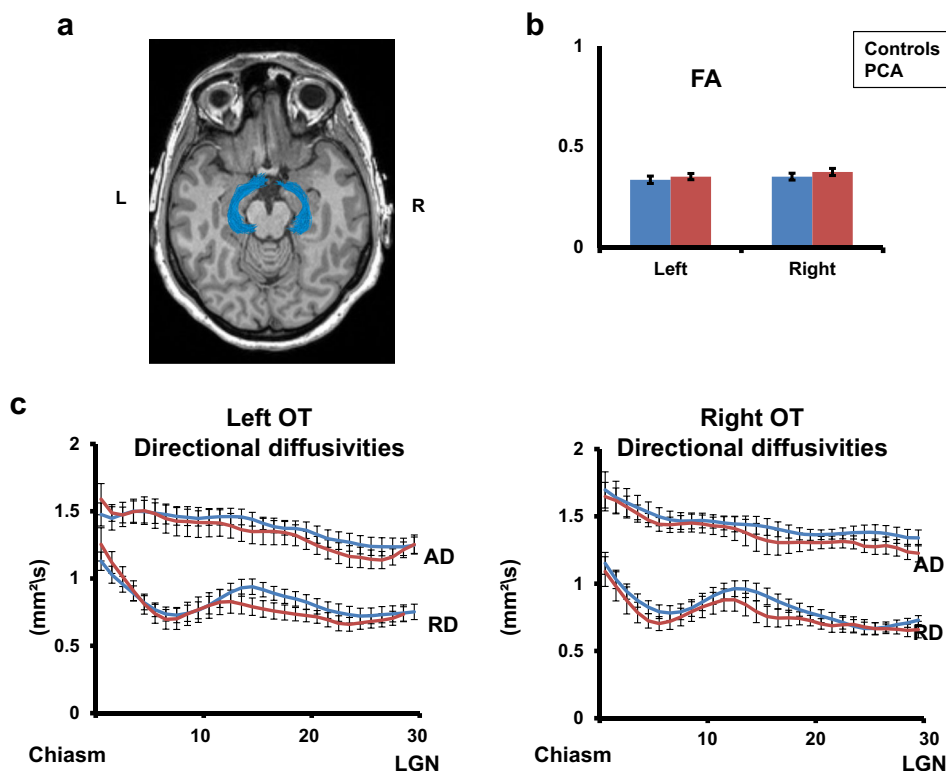
Cluster	Estimated location	Peak	Size	P (FWE)	x	y	z
1	L Ant Occipital		395				
		1		0.001	-27	-92	3
		2		0.008	-35	-87	2
2	R Ant Occipital		1016				
		1		0.001	53	-83	9
		2		0.002	38	-77	21
3	R MT		678				
		1		0.002	53	-29	-11
		2		0.01	45	-24	12

along the occipito-callosal fibers on either side. Thus, similar to the optic radiation, reduced diffusivity was evident in regions adjacent to the occipital cortex. Distant parts of the fiber bundle demonstrated intact diffusivities. Differences were again seen more on the left side and were driven mainly by elevated RD.

A comparison of the relative callosal volume taken by the occipital group revealed no differences between the study cohorts, i.e. the internal organization of the corpus callosum does not differ between patients and controls ($p = 0.37$).

Fig. 2 Optic tracts. a

Visualization of the optic tracts, as delineated via fiber tractography, superimposed on an axial cortical view (b) Averaged fractional anisotropy (FA) of the right and left optic tracts. c Axial diffusivity (AD) and radial diffusivity (RD) profiles along the left and right optic tracts. Error bars represent standard error of the mean



Functional connectivity measurements

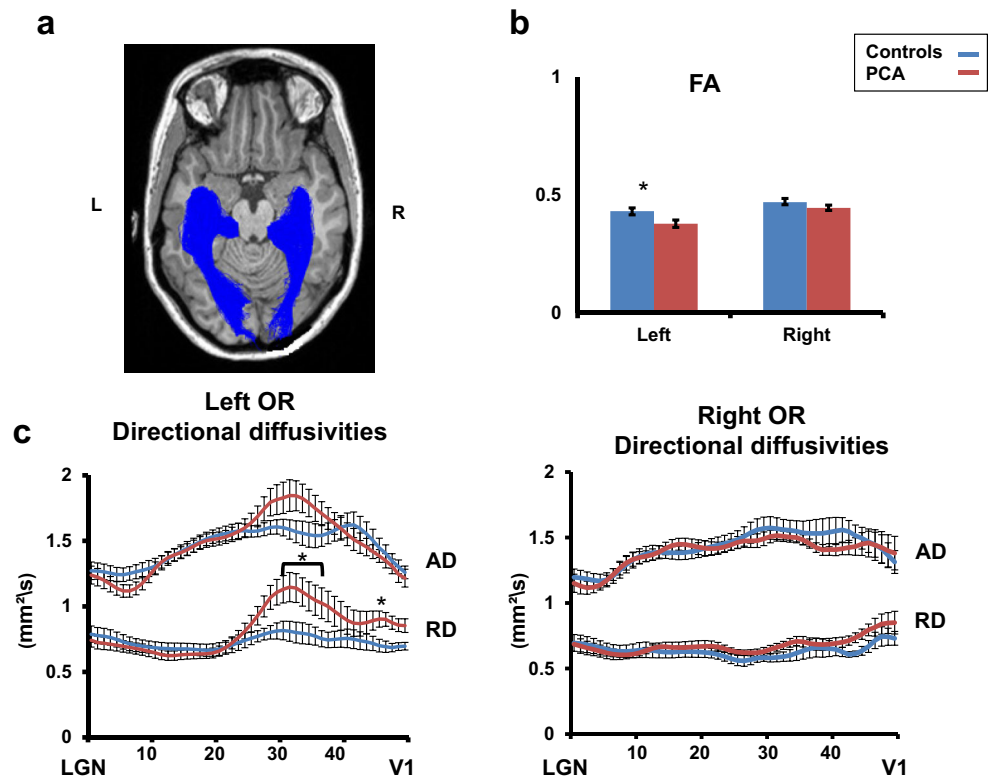
Reduced functional connectivity is seen within the visual network (Fig. 5) Comparison of the primary visual cortex seed-region maps revealed reduced connectivity in PCA patients as compared to controls. Direct comparison of connectivity levels within the pre-defined visual and non-visual regions between patients and controls, revealed significant reduction in connectivity in several high-order visual areas, including the right MT ($p = 0.008$), right LOC ($p = 0.003$) and left LOC ($p = 0.028$), as well as within the entire occipital cortex ($p = 0.04$). Reduction in connectivity was also evident in the left FEF, known to be involved in control of eye movements and visual attention.

Correlations analysis

We first studied the effect of GM atrophy on the behavioral measurements and on the structural and functional connectivity. This resulted in the following significant correlations:

GM volume correlated with spatial perception Total GM volume and the right anterior occipital atrophied focus volume were correlated with spatial perception ($\tau = 0.5$, $p = 0.042$; $\tau = 0.5$, $p = 0.042$). The greater the reduction in GM volume, the worse the spatial perception.

Fig. 3 Optic radiations. **a** Visualization of the optic radiations, as delineated via fiber tractography, superimposed on an axial cortical view. **b** Averaged fractional anisotropy (FA) of the right and left optic radiation. **c** Axial diffusivity (AD) and radial diffusivity (RD) profiles along the left and right optic radiations. Error bars represent standard error of the mean. Black bars indicate area of significant difference between the groups, after correcting for multiple comparisons. * $p < 0.05$



GM volume correlated with diffusivity measures of the occipito-callosal fibers Positive correlations were found between the left anterior occipital focus' volume and the left occipito-callosal fibers' FA ($\tau = 0.643$, $p = 0.013$). Thus preserved GM volume was associated with better integrity of the adjacent occipito-callosal fibers.

GM volume correlated with the connectivity measures of the FEF Significant positive correlations were found between total GM volume and connectivity levels in the *left* FEF ($\tau = 0.619$, $p = 0.025$). Thus preserved GM volume was associated with better synchronization between V1 and the frontal eye fields.

Additionally, we looked at the correlation between the behavioral measurements, and the structural and functional connectivity.

Diffusivity measures in the affected pathways correlated with motion perception (Fig. 6) Significant correlations were found between diffusivity measures in the left optic radiation and left occipito-callosal and motion coherence abilities. Negative correlations were evident between FA and motion perception in both fiber bundles ($\tau = -0.86$, $p = 0.003$; $\tau = -0.64$, $p = 0.013$ for optic radiation and occipito-callosal correspondingly). In accordance, significant positive relationships were evident between the RD and AD values and motion coherence levels (optic radiation: $\tau = 0.71$, $p = 0.007$; $\tau = 0.86$, $p = 0.001$; occipito-callosal fibers: $\tau = 0.57$, $p = 0.02$; $\tau = 0.79$, $p = 0.003$ for RD and AD respectively). Thus, the worse the integrity of

the fiber tract, the worse the ability to identify coherent motion within an array of dots.

When the GM volume was added as a covariant to the analysis, only correlation between the integrity of the left optic radiation and the motion coherence perception remained significant ($\tau = -0.57$, $p = 0.048$; $\tau = 0.57$, $p = 0.048$; FA and RD respectively). The correlation between the occipito-callosal integrity and motion coherence perception was no longer significant ($\tau = -0.25$, $p = 0.46$; $\tau = 0.071$, $p = 0.81$; FA and RD respectively), suggesting that this correlation was, at least partially, GM-dependent.

Discussion

To summarize, WM structural connectivity showed reduced diffusivity, indicating impaired WM integrity along the optic radiations and the splenial fibers, in close proximity to damaged GM areas. Fiber parts which are located far from affected cortical area, i.e. the anterior optic radiation and the callosal portion of the occipito-callosal fibers, were not affected. Furthermore, degeneration did not proceed to the optic tracts, which did not differ in diffusivity parameters from the age-matched group, possibly opposing trans-synaptic changes, at least in the early stages of the disease.

Reductions in functional connectivity were seen in the connections between V1 and higher visual areas, as well as between V1 and the FEF, known to be involved in control of eye

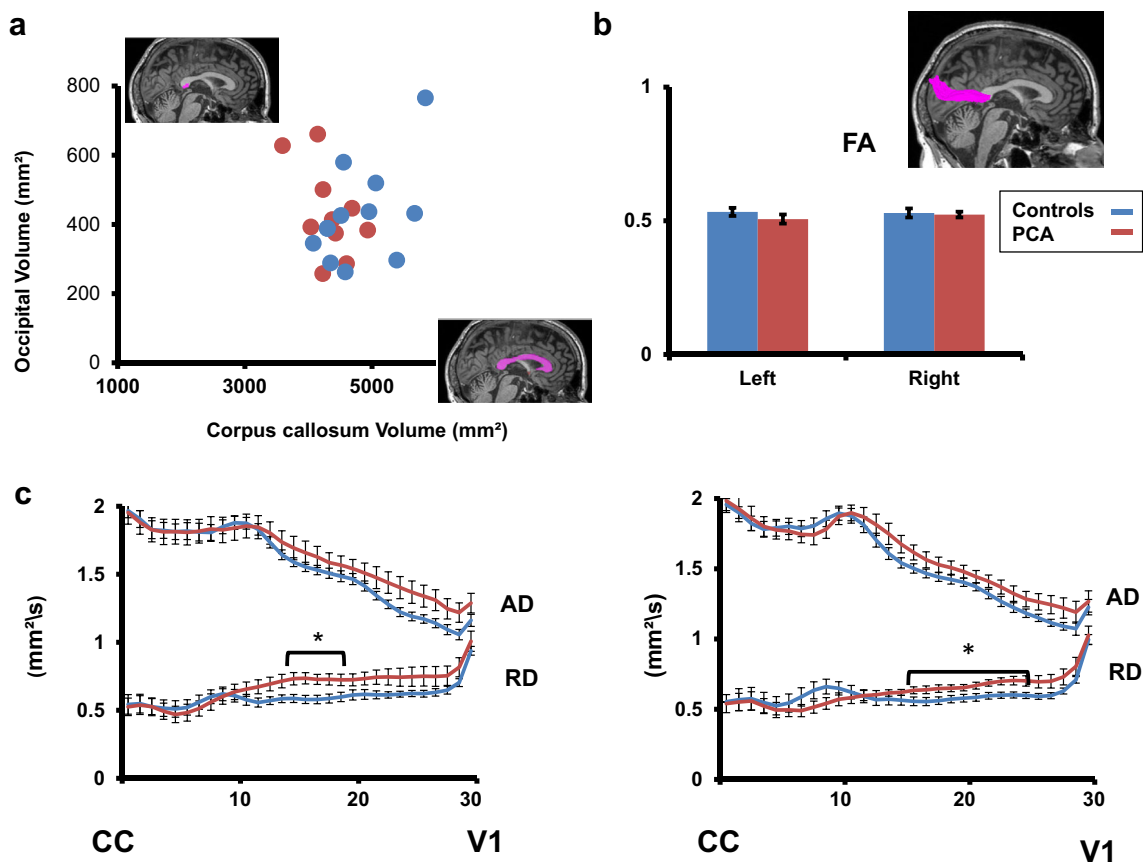


Fig. 4 Occipital callosal (splenial) fibers. **a** The relationship between the volume of splenial-callosal fibers, evaluated over the five mid-sagittal slices, and the volume of the total corpus callosum, evaluated over the same slices, compared between PCA and controls. **b** Averaged fractional anisotropy (FA) of the right and left occipito-callosal fibers (**c**) Axial

diffusivity (AD) and radial diffusivity (RD) profiles along the left and right occipito-callosal fibers. Error bars represent standard error of the mean. Black horizontal bars indicate areas of significance different between the groups, after correcting for multiple comparisons. * $p < 0.05$

movement and visual attention. Structural and functional connectivity reduction was related to volume depletion. Interestingly, correlations were found between the integrity of the affected fibers and patients' motion perception suggesting that fiber integrity plays a role in determining behavioral manifestation.

As was demonstrated by postmortem and in-vivo evidence, and contrary to long-held beliefs, today it is accepted that WM involvement is common in Alzheimer's disease and its variants (for review (Caso et al. 2016)). Putative mechanisms to explain fiber degeneration are divided into theories that are GM-dependent and independent. Example for the latter is degeneration by developmental order (late-myelinating fibers are the first to degenerate). However, assuming that WM damage is the consequence and not the origin of the pathology, local and distant mechanisms were suggested. Protein aggregates might spread locally to adjacent fibers and microglia activation may lead to neurotoxicity but also to oligodendrotoxicity. This local effect can spread distantly, along networks that are anatomically (e.g. *cingulum*) or functionally (e.g. default mode network) defined (Balachandar et al. 2015).

Our DTI results in the PCA variant suggest localized damage. It is important to note that our study focused on the visual pathways. Within this network, no distant effects were evident. However, other studies that either looked at the entire brain, using whole brain template analysis (Caso et al. 2015; Cerami et al. 2015; Madhavan et al. 2015), or delineated the anterior-posterior longitudinal fasciculi (Migliaccio et al. 2012) reported WM involvement within fibers connecting the occipital cortices with temporal and frontal regions, suggesting possible deafferentation processes. No specific studies on the optic tracts and radiations or occipito-callosal fibers lengthwise were previously reported. Thus, we can argue that disease progression along the WM, if exists, evolves along pathways connecting the visual system to other cortical regions and not within the visual pathways themselves.

Functional connectivity deficits in our cohort were observed within the visual network, as compared to healthy controls. These local changes were accompanied by reduction in connectivity to a distant, yet functionally connected, area: the FEF. Changes found in both local and distant functionally connected areas may be partially explained by related volume depletion, in the way that lower activity (as we previously

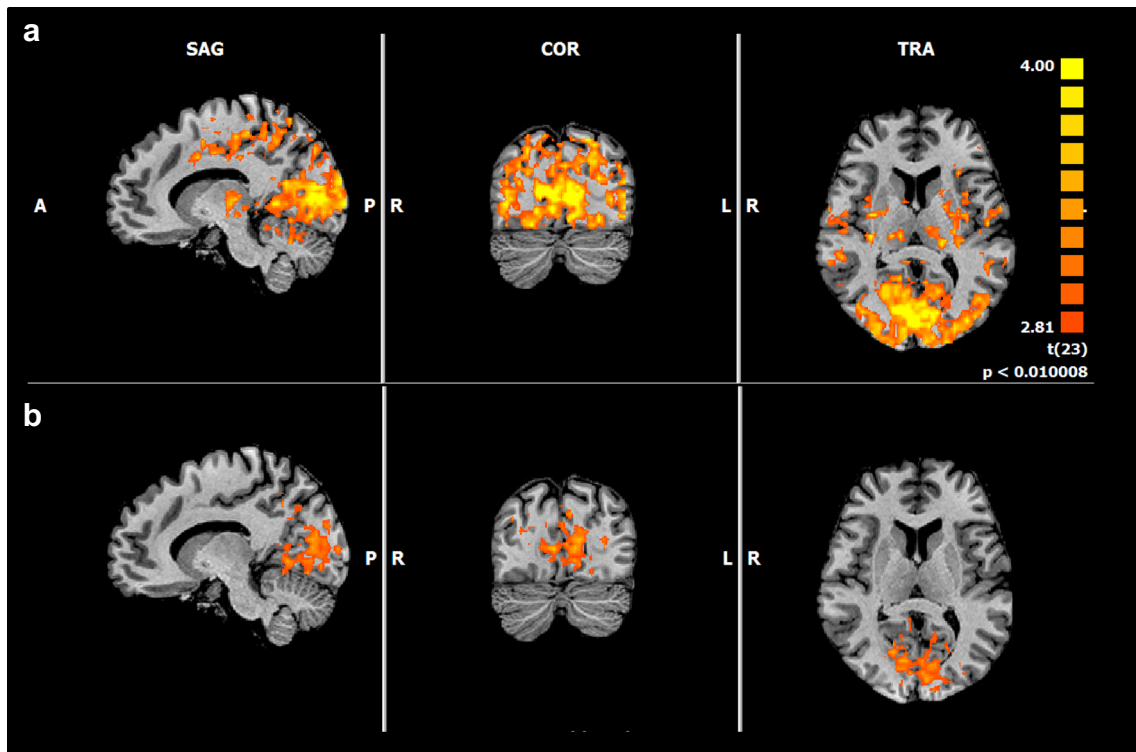
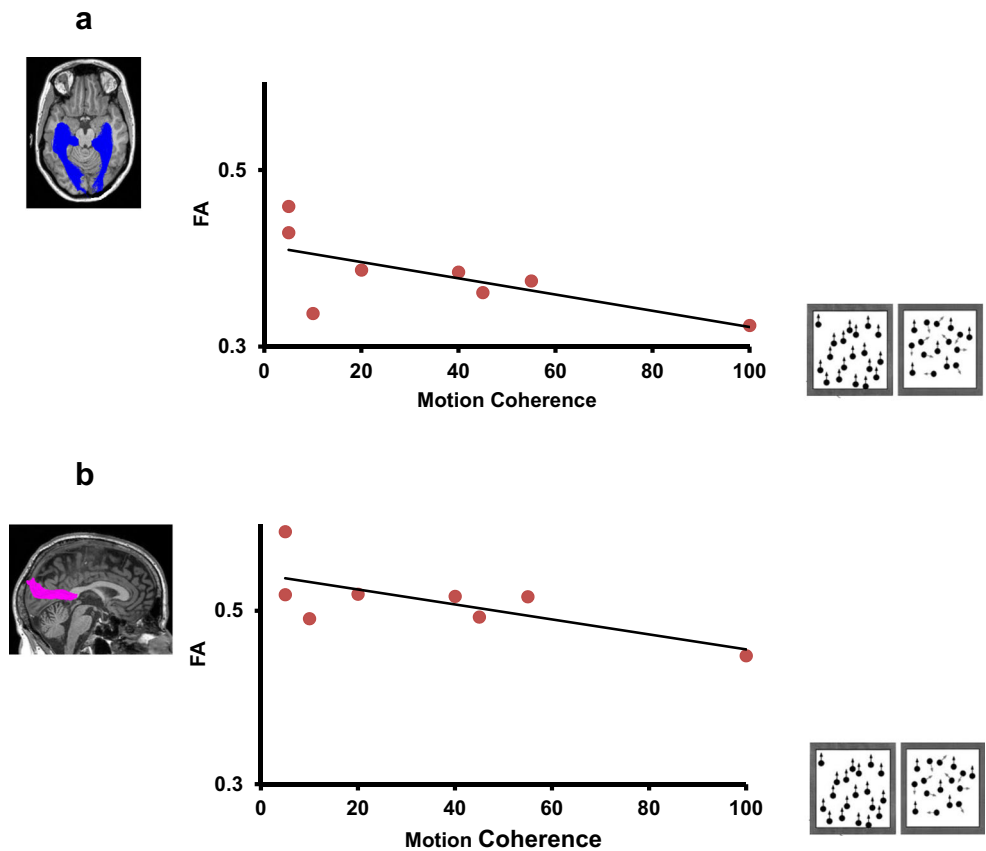


Fig. 5 Visual network functional connectivity. Group visual-network functional connectivity maps in the controls (a) and in PCA patients (b) superimposed on a T1 sagittal, coronal and axial view

Fig. 6 Correlation between fiber integrity and behavioral measurements. Correlation between PCA patients’ ability to perceive motion as tested in the motion coherence test and their fractional anisotropy (FA) measures in optic radiation (a) and occipito-callosal fibers (b)



described (Shames et al. 2015)) in one node of a network affects the connectivity of the entire network. The current findings are in agreement with previous studies that found that reduction in connectivity in degenerative diseases, while related to atrophy, goes beyond it (Son et al. 2017) (Tuovinen et al. 2016; Lehmann et al. 2015).

A relationship between locally measured diffusion parameters and behavioral data as a reflection of structure–function coupling was previously reported in healthy subjects (Johansen-Berg 2010). Specifically, a positive correlation was found between coherent motion detection and local FA in the left parietal WM and in the left optic radiation (Csete et al. 2014).

Our results in PCA subjects further emphasize this structure–function relationship.

The structural determinant could reflect proximity to motion-related cortical areas. High densities of senile plaque and neurofibrillary tangles in the MT area were previously reported in pathological studies, signifying its specific role in the disease (Hof et al. 1997).

Alternatively, the association between motion perception and visual pathways integrity may indicate the need for rapid transmission of visual input along intact fibers, to perceive motion (as we previously suggested in multiple sclerosis (Raz et al. 2012)). In that case WM damage is the origin of the behavioral phenomenon and not a bystander.

Our findings correspond to a recent report (Neitzel et al. 2016) suggesting that reduced visual processing speed explains simultanagnosia in PCA patients and that the left posterior WM degree of atrophy (measured by VBM) predicts this slowing of processing speed.

It is important to note that our findings are based on a cross-sectional study with patients whose symptoms began 4 years or less before the time of evaluation. Thus, our conclusion can be related to the early disease stages and a follow up study is needed.

Another reservation to be noted when discussing the relationship between GM and WM involvement is linked to the available methods' limitations. Diffusivity measurements are not limited to WM and include all elements in the vicinity of the measured voxel.

Thus diffusivity differences which are reported may be driven by atrophy. The choice of probabilistic algorithm and the analysis method focusing on the fiber core were aimed to optimize our results despite the known difficulties (Raz et al. 2015).

To conclude, our results on early PCA patients suggest that WM involvement and network integrity in degenerative disease may be GM-dependent but nevertheless plays a role in determining behavioral manifestation.

Compliance with ethical standards

Author disclosures Haya Glick Shames – Reports no disclosures.

Yael Backner- Reports no disclosures.

Atira Bick - Reports no disclosures.

Noa Raz- Reports no disclosures.

Netta Levin- Reports no disclosures.

Ethics committee The study was approved by the Helsinki Committee of Hadassah Hospital.

Informed consent Informed consent was obtained from all individual participants included in the study.

Ethical approval All procedures performed in studies involving human participants were in accordance with the ethical standards of the institutional and/or national research committee and with the 1964 Helsinki declaration and its later amendments or comparable ethical standards.

References

- Alegret, M., Boada-Rovira, M., Vinyes-Junqué, G., Valero, S., Espinosa, A., Hernández, I., Modinos, G., Rosende-Roca, M., Mauleón, A., Becker, J. T., & Tárraga, L. (2009). Detection of visuo-perceptual deficits in preclinical and mild Alzheimer's disease. *Journal of Clinical and Experimental Neuropsychology*, 31(7), 860–867.
- Alves, J., Soares, J. M., Sampaio, A., & Goncalves, O. F. (2013). Posterior cortical atrophy and Alzheimer's disease: a meta-analytic review of neuropsychological and brain morphometry studies. *Brain Imaging and Behavior*, 7(3), 353–361. <https://doi.org/10.1007/s11682-013-9236-1>.
- Balachandar, R., John, J. P., Saini, J., Kumar, K. J., Joshi, H., Sadanand, S., Aiyappan, S., Sivakumar, P. T., Loganathan, S., Varghese, M., & Bharath, S. (2015). A study of structural and functional connectivity in early Alzheimer's disease using rest fMRI and diffusion tensor imaging. *International Journal of Geriatric Psychiatry*, 30(5), 497–504. <https://doi.org/10.1002/gps.4168>.
- Bartzokis, G. (2004). Age-related myelin breakdown: a developmental model of cognitive decline and Alzheimer's disease. *Neurobiology of Aging*, 25(1), 5–18 author reply 49–62.
- Benson, D. F., Davis, R. J., & Snyder, B. D. (1988). Posterior cortical atrophy. *Archives of Neurology*, 45(7), 789–793.
- Braddick, O., Atkinson, J., & Wattam-Bell, J. (2003). Normal and anomalous development of visual motion processing: motion coherence and 'dorsal-stream vulnerability'. *Neuropsychologia*, 41(13), 1769–1784.
- Burns, J. M., Church, J. A., Johnson, D. K., Xiong, C., Marcus, D., Fotenos, A. F., Snyder, A. Z., Morris, J. C., & Buckner, R. L. (2005). White matter lesions are prevalent but differentially related with cognition in aging and early Alzheimer disease. *Archives of Neurology*, 62(12), 1870–1876. <https://doi.org/10.1001/archneur.62.12.1870>.
- Canu, E., Frisoni, G. B., Agosta, F., Pievani, M., Bonetti, M., & Filippi, M. (2012). Early and late onset Alzheimer's disease patients have distinct patterns of white matter damage. *Neurobiology of Aging*, 33(6), 1023–1033. <https://doi.org/10.1016/j.neurobiolaging.2010.09.021>.
- Caso, F., Agosta, F., Mattavelli, D., Migliaccio, R., Canu, E., Magnani, G., Marcone, A., Copetti, M., Falautano, M., Comi, G., Falini, A., & Filippi, M. (2015). White matter degeneration in atypical Alzheimer disease. *Radiology*, 277(1), 162–172. <https://doi.org/10.1148/radiol.2015142766>.
- Caso, F., Agosta, F., & Filippi, M. (2016). Insights into white matter damage in Alzheimer's disease: from postmortem to in vivo diffusion tensor MRI studies. *Neurodegenerative Diseases*, 16(1–2), 26–33. <https://doi.org/10.1159/000441422>.

- Cerami, C., Crespi, C., Della Rosa, P. A., Dodich, A., Marcone, A., Magnani, G., Coppi, E., Falini, A., Cappa, S. F., & Perani, D. (2015). Brain changes within the visuo-spatial attentional network in posterior cortical atrophy. *Journal of Alzheimer's Disease*, *43*(2), 385–395. <https://doi.org/10.3233/JAD-141275>.
- Crutch, S. J., Schott, J. M., Rabinovici, G. D., Murray, M., Snowden, J. S., van der Flier, W. M., et al. (2017). Consensus classification of posterior cortical atrophy. *Alzheimer's & Dementia*, *13*, 870–884.
- Csete, G., Szabo, N., Rokszin, A., Toth, E., Braunitzer, G., Benedek, G., et al. (2014). An investigation of the white matter microstructure in motion detection using diffusion MRI. *Brain Research*, *1570*, 35–42. <https://doi.org/10.1016/j.brainres.2014.05.006>.
- de la Monte, S. M. (1989). Quantitation of cerebral atrophy in preclinical and end-stage Alzheimer's disease. *Annals of Neurology*, *25*(5), 450–459. <https://doi.org/10.1002/ana.410250506>.
- Della Sala, S., Laiacona, M., Trivelli, C., & Spinnler, H. (1995). Poppelreuter-Ghent's overlapping figures test: its sensitivity to age, and its clinical use. *Archives of Clinical Neuropsychology*, *10*(6), 511–534. [https://doi.org/10.1016/0887-6177\(94\)00049-V](https://doi.org/10.1016/0887-6177(94)00049-V).
- Evans, A. C., Collins, D. L., Mills, S. R., Brown, E. D., Kelly, R. L., & Peters, T. M. (1993). 3D statistical neuroanatomical models from 305 MRI volumes. *1993 IEEE Conference Record Nuclear Science Symposium and Medical Imaging Conference*. 31 Oct–6 Nov 1993, 3, 1813–1817.
- Frisoni, G. B., Pievani, M., Testa, C., Sabatelli, F., Bresciani, L., Bonetti, M., Beltramello, A., Hayashi, K. M., Toga, A. W., & Thompson, P. M. (2007). The topography of grey matter involvement in early and late onset Alzheimer's disease. *Brain*, *130*(Pt 3), 720–730. <https://doi.org/10.1093/brain/awl377>.
- Gollin, E. S. (1960). Developmental studies of visual recognition of incomplete objects. *Perceptual and Motor Skills*, *11*, 289–298. <https://doi.org/10.2466/PMS.11.7.289-298>.
- Gress, D. R. (2001). Aging and dementia: more gray hair and less gray matter. *AJNR. American Journal of Neuroradiology*, *22*(9), 1641–1642.
- Greve, K. W., Lindberg, R. F., Bianchini, K. J., & Adams, D. (2000). Construct validity and predictive value of the Hooper visual organization test in stroke rehabilitation. *Applied Neuropsychology*, *7*(4), 215–222. https://doi.org/10.1207/S15324826AN0704_3.
- Hof, P. R., Vogt, B. A., Bouras, C., & Morrison, J. H. (1997). Atypical form of Alzheimer's disease with prominent posterior cortical atrophy: a review of lesion distribution and circuit disconnection in cortical visual pathways. *Vision Research*, *37*(24), 3609–3625. [https://doi.org/10.1016/S0042-6989\(96\)00240-4](https://doi.org/10.1016/S0042-6989(96)00240-4).
- Huang, H., Zhang, J., Jiang, H., Wakana, S., Poetscher, L., Miller, M. I., van Zijl, P. C. M., Hillis, A. E., Wytko, R., & Mori, S. (2005). DTI tractography based parcellation of white matter: application to the mid-sagittal morphology of corpus callosum. *NeuroImage*, *26*(1), 195–205. <https://doi.org/10.1016/j.neuroimage.2005.01.019>.
- Johansen-Berg, H. (2010). Behavioural relevance of variation in white matter microstructure. *Current Opinion in Neurology*, *23*(4), 351–358. <https://doi.org/10.1097/WCO.0b013e32833b7631>.
- Kaesler, P. F., Ghika, J., & Borruat, F. X. (2015). Visual signs and symptoms in patients with the visual variant of Alzheimer disease. *BMC Ophthalmology*, *15*, 65. <https://doi.org/10.1186/s12886-015-0060-9>.
- Lacadie, C. M., Fulbright, R. K., Constable, R. T., & Papademetris, X. (2008). More accurate Talairach coordinates for neuroImaging using nonlinear registration. *NeuroImage*, *42*(2), 717–725. <https://doi.org/10.1016/j.neuroimage.2008.04.240>.
- Lehmann, M., Madison, C., Ghosh, P. M., Miller, Z. A., Greicius, M. D., Kramer, J. H., Coppola, G., Miller, B. L., Jagust, W. J., Gorno-Tempini, M. L., Seeley, W. W., & Rabinovici, G. D. (2015). Loss of functional connectivity is greater outside the default mode network in nonfamilial early-onset Alzheimer's disease variants. *Neurobiology of Aging*, *36*(10), 2678–2686. <https://doi.org/10.1016/j.neurobiolaging.2015.06.029>.
- Liberman, J., Stewart, W., Seines, O., & Gordon, B. (1994). Rater agreement for the Rey-Osterrieth complex figure test. *Journal of Clinical Psychology*, *50*(4), 615–624.
- Madhavan, A., Schwarz, C. G., Duffy, J. R., Strand, E. A., Machulda, M. M., Drubach, D. A., Kantarci, K., Przybelski, S. A., Reid, R. I., Senjem, M. L., Gunter, J. L., Apostolova, L. G., Lowe, V. J., Petersen, R. C., Jack, C. R., Josephs, K. A., & Whitwell, J. L. (2015). Characterizing white matter tract degeneration in syndromic variants of Alzheimer's disease: a diffusion tensor imaging study. *Journal of Alzheimer's Disease*, *49*(3), 633–643. <https://doi.org/10.3233/JAD-150502>.
- Migliaccio, R., Agosta, F., Scola, E., Magnani, G., Cappa, S. F., Pagani, E., Canu, E., Comi, G., Falini, A., Gorno-Tempini, M. L., Bartolomeo, P., & Filippi, M. (2012). Ventral and dorsal visual streams in posterior cortical atrophy: a DT MRI study. *Neurobiology of Aging*, *33*(11), 2572–2584. <https://doi.org/10.1016/j.neurobiolaging.2011.12.025>.
- Neitzel, J., Ortner, M., Haupt, M., Redel, P., Grimmer, T., Yakushev, I., Drzezga, A., Bublak, P., Preul, C., Sorg, C., & Finke, K. (2016). Neuro-cognitive mechanisms of simultanagnosia in patients with posterior cortical atrophy. *Brain*, *139*(Pt 12), 3267–3280. <https://doi.org/10.1093/brain/aww235>.
- Pillon, B., Dubois, B., Bonnet, A., Esteguy, M., Guimaraes, J., Vigouret, J., et al. (1989). Cognitive slowing in Parkinson's disease fails to respond to levodopa treatment the 15-objects test. *Neurology*, *39*(6), 762–762.
- Raz, N., Dotan, S., Chokron, S., Ben-Hur, T., & Levin, N. (2012). Demyelination affects temporal aspects of perception: an optic neuritis study. *Annals of Neurology*, *71*(4), 531–538. <https://doi.org/10.1002/ana.22692>.
- Raz, N., Bick, A. S., Ben-Hur, T., & Levin, N. (2015). Focal demyelination damage and neighboring white matter integrity: an optic neuritis study. *Multiple Sclerosis*, *21*(5), 562–571. <https://doi.org/10.1177/1352458514551452>.
- Reiner, A., Yekutieli, D., & Benjamini, Y. (2003). Identifying differentially expressed genes using false discovery rate controlling procedures. *Bioinformatics*, *19*(3), 368–375.
- Shames, H., Raz, N., & Levin, N. (2015). Functional neural substrates of posterior cortical atrophy patients. *Journal of Neurology*, *262*(7), 1751–1761. <https://doi.org/10.1007/s00415-015-7774-8>.
- Sherbondy, A. J., Dougherty, R. F., Ben-Shachar, M., Napel, S., & Wandell, B. A. (2008). ConTrack: finding the most likely pathways between brain regions using diffusion tractography. *Journal of Vision*, *8*(15), 1–16. <https://doi.org/10.1167/8.9.15>.
- Shin, M.-S., Park, S.-Y., Park, S.-R., Seol, S.-H., & Kwon, J. S. (2006). Clinical and empirical applications of the Rey–Osterrieth complex figure test. *Nature Protocols*, *1*(2), 892–899.
- Son, S. J., Kim, J., & Park, H. (2017). Structural and functional connective fingerprints in mild cognitive impairment and Alzheimer's disease patients. *PLoS One*, *12*(3), e0173426. <https://doi.org/10.1371/journal.pone.0173426>.
- Tamkin, A. S., & Jacobsen, R. (1984). Age-related norms for the Hooper visual organization test. *Journal of Clinical Psychology*, *40*(6), 1459–1463.
- Tuovinen, T., Rytty, R., Moilanen, V., Abou Elseoud, A., Veijola, J., Remes, A. M., & Kiviniemi, V. J. (2016). The effect of gray matter ICA and coefficient of variation mapping of BOLD data on the detection of functional connectivity changes in Alzheimer's disease and bvFTD. *Frontiers in Human Neuroscience*, *10*, 680. <https://doi.org/10.3389/fnhum.2016.00680>.
- Yeatman, J. D., Dougherty, R. F., Myall, N. J., Wandell, B. A., & Feldman, H. M. (2012). Tract profiles of white matter properties: automating fiber-tract quantification. *PLoS One*, *7*(11), e49790. <https://doi.org/10.1371/journal.pone.0049790>.